

A grip force model for the da Vinci end-effector to predict a compensation force

Chiwon Lee · Yong Hyun Park · Chiyul Yoon ·
Seungwoo Noh · Choonghee Lee · Youdan Kim ·
Hee Chan Kim · Hyeon Hoe Kim · Sungwan Kim

Received: 26 March 2013 / Accepted: 16 November 2014 / Published online: 29 November 2014
© International Federation for Medical and Biological Engineering 2014

Abstract A torque transfer system (TTS) that measures grip forces is developed to resolve a potential drawback of the current da Vinci robot system whose grip forces vary according to the different postures of its EndoWrist. A preliminary model of EndoWrist Inner Mechanism Model (EIMM) is also developed and validated with real grip force measurements. EndoWrist's grip forces, posture angles, and transferred torque are measured by using TTS. The mean measured grip forces of three different EndoWrist for 27 different postures were very diverse. The EndoWrist exerted different grip forces, with a minimum of 1.84-times more and a maximum of 3.37-times more in specific posture even if the surgeon exerted the same amount of force. Using the posture angles as input and the grip forces as output, the EIMM is constructed. Then, expected grip force values obtained from EIMM are compared with actual measurements of da Vinci EndoWrist to validate the proposed model. From these results, surgeons will be beneficial with the understandings of actual grip force being applied to tissue and mechanical properties

of robotic system. The EIMM could provide a baseline in designing a force-feedback system for surgical robot. These are significantly important to prevent serious injury by maintaining a proper force to tissue.

Keywords Surgical instruments · Laparoscopy · da Vinci end-effector · Grip force modeling · Compensation force

Abbreviations

TTS	Torque transfer system
EIMM	EndoWrist Inner Mechanism Model
NI	National instruments
PF	Prograsp forceps
PDF	PK dissecting forceps
LND	Large needle driver
SD	Standard deviation
CT	Coupled terms
HOT	High-order term
MGF	Mean grip force
SEM	Standard error of measurement

C. Lee · C. Yoon · S. Noh · C. Lee
The Interdisciplinary Program for Bioengineering, Graduate
School, Seoul National University, Seoul 110-744, Korea
e-mail: lcwkf16@snu.ac.kr

C. Yoon
e-mail: chiyul@melab.snu.ac.kr

S. Noh
e-mail: tarzan@melab.snu.ac.kr

C. Lee
e-mail: lch2722@snu.ac.kr

Y. H. Park · H. H. Kim
Department of Urology, Seoul National University Hospital,
Seoul 110-744, Korea
e-mail: lestat04@empas.com

H. H. Kim
e-mail: hhkim@snu.ac.kr

Y. Kim
Department of Mechanical and Aerospace Engineering, Seoul
National University College of Engineering, Seoul 151-742,
Korea
e-mail: ydkim@snu.ac.kr

H. C. Kim · S. Kim (✉)
Department of Biomedical Engineering, Institute of Medical
and Biological Engineering, Seoul National University,
Seoul 110-799, Korea
e-mail: sungwan@snu.ac.kr

1 Introduction

The usage of robots in surgical procedures is rapidly increasing. The key advantages of robot-assisted surgery over conventional open surgery are a small incision area, a smaller quantity of blood loss, and low infection rates which eventually speed-up the patient's recovery [6, 12, 13, 17]. The market-leading surgical robotics system, the da Vinci (Intuitive Surgical, Inc., Sunnyvale, CA, USA), has demonstrated its safety and efficacy in laparoscopic surgery. The number of operations performed with the da Vinci rapidly increases every year, and the types of surgeries that the da Vinci can perform are expanding into urology, obstetrics, and gynecology [7].

One reason that da Vinci system has been able to successfully perform a wide range of surgeries is its unique design of end-effectors, EndoWrist, which are designed to allow surgeons to easily control the robot's movements [6]. In the EndoWrist, four strings are connected to each servo motor in robot arm of the da Vinci; a surgeon's delicate hand movements can be reproduced inside the human body while minimizing the diameters of the opening ports.

However, in the current image-guided system for the da Vinci robot system, which has no haptic technology and no feedback on the grip forces, a wide range of different grip forces are observed with respect to the various postures of EndoWrist [12]. During the robotic surgery, surgeons do not realize that varying forces are being applied to the end-effector, because the system is an image-guided system; therefore, excessive mechanical force could be applied to cause the breakage of end-effector string (Fig. 1) or could cause serious tissue injury, such as cutting arteries or nerves [3, 10, 14, 18].

The variation in forces according to the EndoWrist's postures is caused by the current end-effector's structure and design. The torque or the force from the motor could not be transferred to the end-effector's gripper intact because of the friction and the interference among the four strings inside the end-effector [16]. To calculate the amount of grip force that is required to compensate for an excessive or insufficient force, the relationship between the EndoWrist's position (posture) and the force transferred to the EndoWrist's gripper need to be determined; however, only limited and quantitative force difference was proven [12], and in-depth theoretical analyses of the excessive or insufficient force has not been previously conducted [5].

In this research, the EndoWrist Inner Mechanism Model (EIMM) is developed to quantitatively and theoretically analyze the EndoWrist's grip force. The EndoWrist's grip forces, posture angles, and transferred torque are measured using the torque transfer system (TTS), which is proposed in this study. There are some differences between surgeon's control for the master interface of da Vinci system and our

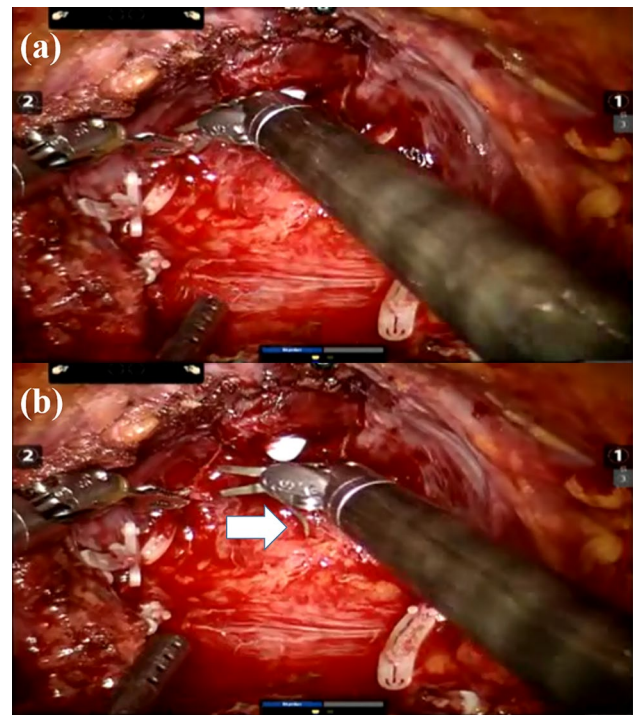


Fig. 1 **a** The small clip applicator was bent to ligate the small artery (normal state). **b** The small clip applicator suddenly became loose because of a broken string (failure state)

proposed automatic triggering method. The da Vinci robot's torque transfer mechanism to EndoWrist is different from our proposed TTS since the TTS is directly driven by four motors with minimal mechanical strings for allowing TTS to exert comparable grip force with da Vinci system using only small capacity motor. However, since the surgeon's intention for the massive or tiny grip force could not be transferred to slave end-effector, EndoWrist [9], there are no problem to apply TTS to EndoWrist's movement modeling. Using the posture angles as the input and the grip forces as the output, a model of the EndoWrist's inner mechanism is developed. Next, the values of expected grip force obtained from the model are compared with actual measurements from da Vinci EndoWrist to verify and validate the model.

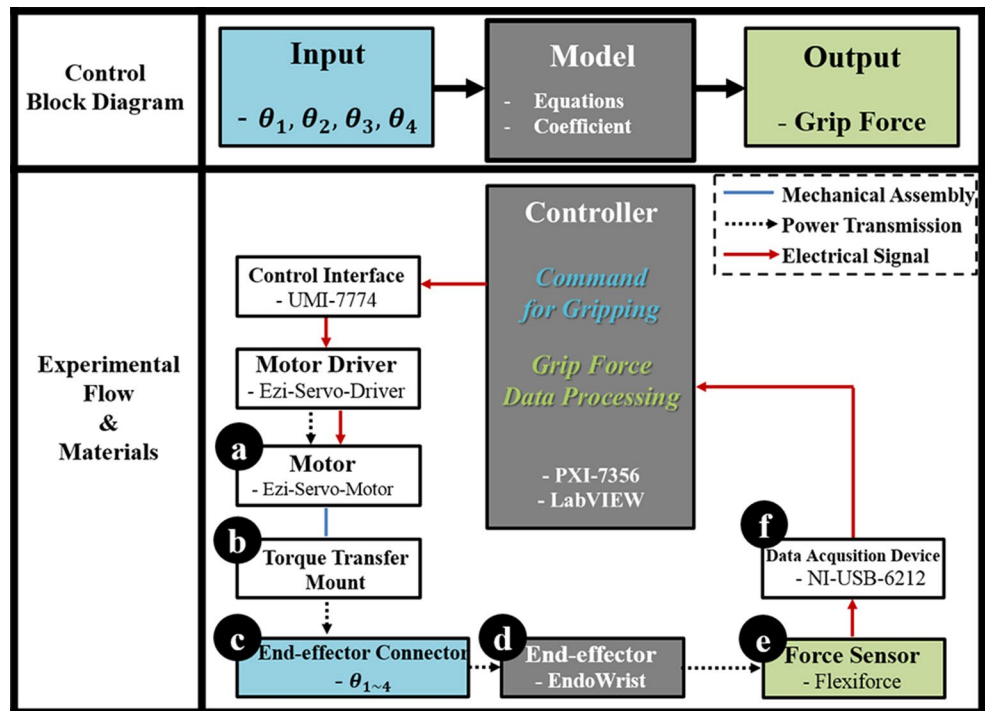
These methods are presented in Sects. 2 and 3. Section 4 describes Discussion followed by Conclusions in Sect. 5.

2 Materials and methods

2.1 Development of the torque transfer system (TTS)

A control block diagram for the EIMM is shown in Fig. 2. The input variable for the EIMM was the EndoWrist's posture angles (θ_1 , θ_2 , θ_3 , θ_4), and the output variable was the EndoWrist's grip force. Using the input and output

Fig. 2 Control block diagram and experimental flow for the torque transfer system (TTS). A da Vinci end-effector (EndoWrist) is mounted on the in-house torque transfer mount (b) and four motors (a) controlling the EndoWrist (d). Gripping forces are measured using a piezoresistive sensor (e) through the specific electric circuit and data acquisition device (f) in accordance with the roll (α), pitch (β), and yaw (γ) movements of the EndoWrist



variables, the unknown system of the EndoWrist's inner mechanism was identified using modeling techniques.

The da Vinci system used four servo motors to control the movement of the EndoWrist. To provide conditions similar to da Vinci's operation, the TTS, which was composed of motors, connectors, an in-house mount kit, and a controller, was developed as depicted in Figs. 2 and 3. In the TTS, the four motors were the major torque power source. High-resolution, closed-loop controlled motors (Ezi-Servo-28L-D, Fastech, Bucheon City, GyeongGi-Do, Republic of Korea) were used to achieve a precision control for the EndoWrist. A motor controller [PXI-7356 and UMI-7774, National Instruments (NI), Austin, TX, USA] and software (NI, LabVIEW) were used to control the motors.

The output variable of the grip force was measured using a sensor that was placed between a pair of grippers, as shown in Fig. 3e. A flexible, piezoresistive sensor (Flexiforce, Tekscan Inc., South Boston, MA, USA) was connected to a simple voltage-dividing circuit. Because the sensor changes its resistance according to the applied forces, the voltage across the sensor varied when the gripper grabs an object. For the acquisition of the signal, NI hardware (USB-6212) was used.

2.2 Calibration of the motor/force sensor

A torque sensor (DynPick, Wacoh-Tech Inc., Takaoka City, Futatsuka, Japan) was connected to the EndoWrist's connectors, which were connected to the shaft of the motor. The transferred torque exerted from the motor on

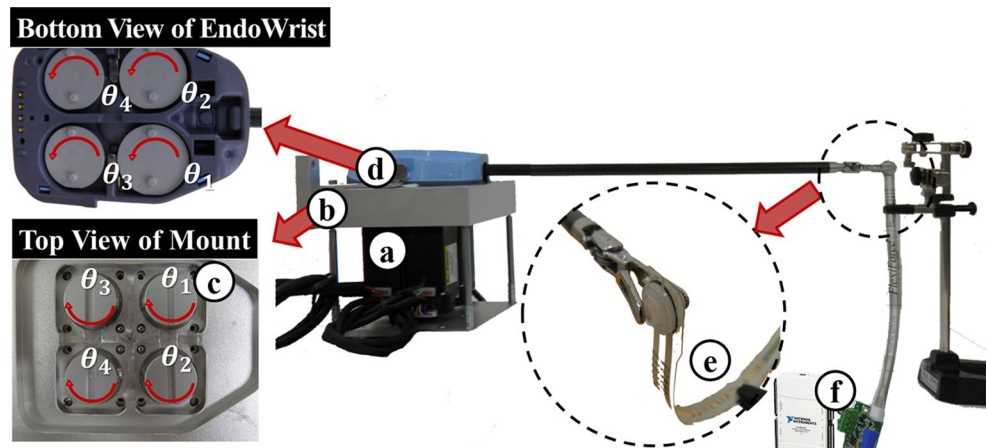
the EndoWrist was measured. The voltage reading of the torque sensor in accordance with the applied torque, and the linear relationship between the torque (T) and the voltage (output voltage of the torque sensor, V_T), was formulated as Eq. (1). Note that the DC offset could be eliminated by reading the sensor value [the mean calculated from ten measurements: 0.2503 N m, standard deviation (SD): 0.0031 N m] during the pre-load condition, and the voltage coefficients were obtained from the sensor's datasheet.

$$T = \frac{V_T - 8192}{819} - 0.2503 \quad (1)$$

Using the Eq. (1), the torque was measured ten times, while the motor was fixed in place. The torque measurement of 0.0838 N m (SD: 0.0032 N m) was exerted constantly from both sides of the gripper. This torque value was lower than the torque value for the da Vinci servo motor (RE25-118751, value: 0.218 N m, Maxon Motors, Brünigstrasse, Sachseln, Switzerland) [8, 15]. However, the measured grip force (4.20 N–20.33 N) was close to the da Vinci grip force (5.52 N–21.64 N) [12] because the da Vinci TTS used string in da Vinci robot arm, which reduced the torque because of strings' interference, while the TTS was driven directly from the motor. Additionally, because the torque sensor was a six-axis electrostatic capacitor type, the optimal experimental condition could be found using the sensor's results while the force (x , y , and z) and torque (x and y) were maintained at zero.

The linearity of the grip force sensor was calibrated with metal weights. The voltage readings of the sensor

Fig. 3 Experimental set-up for the measurement of grip forces inside the torque transfer mount. The parameters θ_1 and θ_2 are involved in the roll (α) and pitch (β) motions, respectively. The parameters θ_3 and θ_4 perform the yaw (γ) motion together



(output voltage of the force sensor, V_F) were plotted against the varying metal weight numbers. All the measurements were repeated ten times, and their mean values were interpolated in Eq. (2) using a first-order regression [11] as the sensor's data-sheet. The SD of the plotted data with Eq. (2) was 2.21 %.

$$F = 11.3122 \times V_F - 3.0713 \quad (2)$$

2.3 Force measurement with respect to the EndoWrist's posture

The analysis of the grip force and its measurement was performed with three different EndoWrist; the prograsp forceps (PF), the PK dissecting forceps (PDF), and the large needle driver (LND). The input factors for controlling the EndoWrist were the angles of connectors (θ_1 , θ_2 , θ_3 , θ_4) shown in the bottom view of EndoWrist (Fig. 3). The parameters θ_1 and θ_2 were involved in the roll (α) and pitch (β , proximal wrist joint movement) motions, respectively, as shown in Fig. 4a. The parameters θ_3 and θ_4 performed the yaw (γ , distal wrist joint movement) motion together. When θ_3 and θ_4 move in the opposite direction, the end-effector's gripper operates open or closed. The relationship between the motor connector angle (θ_1 , θ_2 , θ_3 , θ_4) and the Euler angle (α , β , γ) was empirically calculated using Eqs. (3–5). However, in this paper, because Euler angles were intuitive for surgeons, the roll (α), pitch (β), and yaw (γ) angles can be used instead of da Vinci EndoWrist's connector angle (θ_1 , θ_2 , θ_3 , θ_4).

$$\theta_1 = -\frac{11}{18}\alpha \quad (3)$$

$$\theta_2 = -\frac{13}{14}\beta \quad (4)$$

$$\theta_{3,4} = \gamma - \frac{9}{14}\beta \quad (5)$$

The EndoWrist's roll (α), pitch (β), and yaw (γ) joints are located at different positions, as shown in Fig. 4a. A unique set of Euler angles gives a specific, fixed posture for the EndoWrist. The movement ranges of the Euler angle $A(\alpha, \beta, \gamma)$ in this case are $-270^\circ < \alpha < 270^\circ$, $-70^\circ < \beta < 70^\circ$, and $-90^\circ < \gamma < 90^\circ$, respectively, where $A(\alpha, \beta, \gamma)$ stands for the posture with Euler angle set (α, β, γ). For this research, the angles were selected separately using three steps for α , β , and γ whose values are $(-90^\circ, 0^\circ, 90^\circ)$, $(-70^\circ, 0^\circ, 70^\circ)$, and $(-90^\circ, 0^\circ, 90^\circ)$, respectively. Therefore, a multiple analysis of variance ($3 \times 3 \times 3$) was used, and Euler angles $A(\alpha, \beta, \gamma)$ was expressed as 27 postures of EndoWrist as shown in Table 1. The grip force was measured 5 times for each combination, which represents 27 postures. To understand the relationship between Euler angles and posture, four representative postures were illustrated as shown in Fig. 5. The consistency of measured grip forces for three different EndoWrist was estimated using the standard error of measurement (SEM) [2]. To estimate the SEM, the value of one subtract the reliability coefficient is taken, and the SD of the experiments are multiplied by the square root of this value [1]. The SEM indicated measurement error with the same unit as the original measurement. A true difference between the measurement value and an error of measurement could be discriminated by SEM. To evaluate the consistency of 5 times of grip force measurements for the 27 postures, Cronbach's alpha was used as the reliability coefficient for SEM among the several reliability definitions. The SPSS (IBM Corporation, Armonk, NY, USA) was used for computing Cronbach's alpha [4]. The MATLAB software (The Mathwork, Inc., Natick, MA, USA) was used for calculating SEM.

2.4 EndoWrist Inner Mechanism Model

To quantitatively model EndoWrist's inner mechanism, the formulas shown in Eqs. (6–8) were proposed in this study.

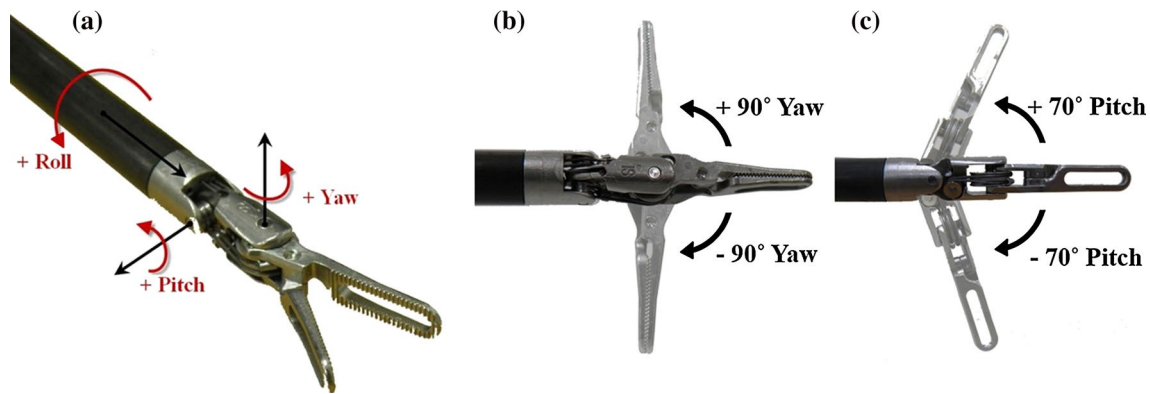


Fig. 4 Orientation of the EndoWrist. By moving the connectors (Fig. 3c), the EndoWrist's orientation and posture are determined. **a** Isometric view. **b** Top view. **c** Side view. According to (a), the

EndoWrist's roll (α), pitch (β), and yaw (γ) orientations are located at different geometrical structures

$$F = C \cdot f(\alpha, \beta, \gamma) \quad (6)$$

$$F = C_0 + C_\alpha \cdot \alpha + C_\beta \cdot \beta + C_\gamma \cdot \gamma + CT + HOT \quad (7)$$

$$\cong [C_0 \ C_\alpha \ C_\beta \ C_\gamma] [1 \ \alpha \ \beta \ \gamma]^T$$

$$\begin{pmatrix} F_{M1} \\ F_{M2} \\ F_{M3} \\ F_{M4} \end{pmatrix} = \begin{pmatrix} 1 & \alpha_1 & \beta_1 & \gamma_1 \\ 1 & \alpha_2 & \beta_2 & \gamma_2 \\ 1 & \alpha_3 & \beta_3 & \gamma_3 \\ 1 & \alpha_4 & \beta_4 & \gamma_4 \end{pmatrix} \begin{pmatrix} C_0 \\ C_\alpha \\ C_\beta \\ C_\gamma \end{pmatrix} \quad (8)$$

The real grip force (F) is shown in Eq. (6) where C and $f(\alpha, \beta, \gamma)$ are unknown coefficients and unknown function of Euler angles, respectively. Next, Eq. (6) was rewritten as a summation of zero-order, first-order, coupled terms (CT), and high-order term (HOT); then, it was simplified with zero-order and first-order terms, as shown in Eq. (7). In this study, a simplified, first-order model was investigated, and the CT and/or HOT will be added if the first-order model is inadequate.

A grip force for the 27 Euler angle combinations was measured, and then, 4 out of the 27 measured grip forces ($F_{M1}, F_{M2}, F_{M3}, F_{M4}$) were used to compute the four unknown coefficients ($C_0, C_\alpha, C_\beta, C_\gamma$) shown in Eq. (8). The 23 remaining measured grip forces were used for validation. In this way, ${}_{27}C_4$, which is 17,750 sets of coefficients, are obtained, and 17,750 sets were analyzed.

3 Results

3.1 Grip force

For the 27 cases for each EndoWrist, the grip forces were measured 5 times, and the mean grip force (MGF) and the SD were computed (Table 1). The overall MGF and the overall SD for the PF EndoWrist were 15.30 N and 0.35 N,

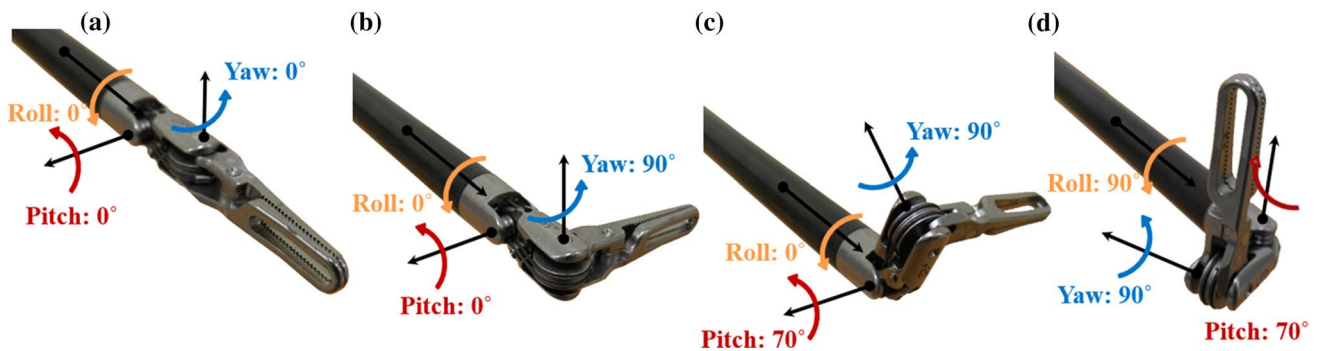
respectively. The overall mean (and SD) of PDF and LND EndoWrist was measured in 7.87 N (0.13 N) and 11.65 N (0.27 N), respectively. The ratio of the SD to the MGF had a minimum of 1.65 % (in PDF) and a maximum of 2.32 % (in LND). As a result, the experimental set-up and the measurement process were acceptable for test. However, it was observed that the MGF for the 27 cases was significantly different. The PF EndoWrist was measured at 20.33 N in $A(0^\circ, 0^\circ, -90^\circ)$ and 11.05 N in $A(0^\circ, 70^\circ, -90^\circ)$. The LND was measured at 17.73 N in $A(90^\circ, 70^\circ, -90^\circ)$ and 6.81 N in $A(0^\circ, 70^\circ, 0^\circ)$. In particular for the PDF EndoWrist, the MGF for two different postures $A(90^\circ, 70^\circ, -90^\circ)$ and $A(-90^\circ, 70^\circ, 90^\circ)$ was 14.15 N and 4.20 N, respectively. These results imply that the EndoWrist exerts a different grip force for a minimum of 1.84 times more (in PF) and a maximum of 3.37 times more (in PDF) in each posture, even if the surgeon exerts the same amount of force. The maximum and minimum values of MGF were observed most frequently at the yaw angles of 90° and -90° .

The LND's measured grip force results among the three EndoWrist used in this study were directly comparable with the reference's results using the actual da Vinci [12]. They conducted the research for the five postures (Neutral, Minor Deflection Right, Minor Deflection Left, Major Deflection Up, and Major Deflection Down), and they were corresponded with Euler angle sets $[(0^\circ, 0^\circ, 0^\circ), (0^\circ, 0^\circ, 90^\circ), (0^\circ, 0^\circ, -90^\circ), (0^\circ, 70^\circ, 0^\circ), \text{ and } (0^\circ, -70^\circ, 0^\circ)]$, which was proposed in this study, respectively. The grip forces for the posture of $(0^\circ, 0^\circ, 90^\circ)$ /'Minor Deflection Right' were slightly bigger than that of the posture of $(0^\circ, 0^\circ, 0^\circ)$ /'Neutral'. These values were slightly smaller than the grip force for the posture of $(0^\circ, 0^\circ, -90^\circ)$ /'Minor Deflection Left'. These three postures' grip forces had similar results. The grip forces for the posture of $(0^\circ, 70^\circ, 0^\circ)$ /'Major Deflection Up' had the smallest value in

Table 1 Measured grip forces for three different EndoWrists

Angle (°)			Mean grip force (N) and standard deviation (N)					
Roll (α)	Pitch (β)	Yaw (γ)	PF		PDF		LND	
			MGF	SD	MGF	SD	MGF	SD
−90	−70	−90	12.12	0.20	5.34	0.14	11.68	0.15
		0	13.28	0.18	5.46	0.05	11.59	0.11
		90	17.28	0.35	4.93	0.06	10.33	0.48
	0	−90	16.68	0.77	4.62	0.04	12.95	0.22
		0	18.98	0.21	5.25	0.10	14.66	0.24
		90	14.35	0.35	6.83	0.09	11.69	0.27
	70	−90	19.15	0.40	5.28	0.03	11.79	0.18
		0	15.95	0.35	5.22	0.06	9.47	0.11
		90	11.58	0.40	4.20	0.08	9.00	0.11
	0	−90	11.62	0.26	10.64	0.23	16.14	1.21
		0	15.50	0.25	6.64	0.08	8.86	0.06
		90	17.73	0.22	6.16	0.09	10.48	0.22
0	−70	−90	20.33	0.31	7.33	0.07	12.00	0.12
		0	16.26	0.53	6.01	0.13	10.57	0.14
		90	15.41	0.54	8.08	0.24	11.67	0.40
	70	−90	11.05	0.21	11.5	0.10	15.12	0.34
		0	13.21	0.35	7.42	0.02	6.81	0.38
		90	13.63	0.36	6.72	0.18	12.52	0.58
	0	−90	14.94	0.27	9.26	0.11	11.41	0.12
		0	15.39	0.27	9.06	0.15	12.85	0.14
		90	14.92	0.46	6.25	0.14	7.17	0.09
	70	−90	17.02	0.51	12.10	0.08	9.89	0.26
		0	15.62	0.38	11.15	0.17	13.92	0.27
		90	14.86	0.34	12.18	0.48	11.99	0.16
90	−70	−90	13.94	0.23	14.15	0.28	17.73	0.38
		0	18.83	0.37	10.79	0.14	13.41	0.25
		90	13.51	0.25	10.02	0.28	8.82	0.21
	0	−90	20.33		14.15		17.73	
		0	11.05		4.20		6.81	
		90	15.30	0.35	7.87	0.13	11.65	0.27
	70	−90	0.99		1.00		0.99	
		0	0.02		0.00		0.01	
		90						
	90	−90						
		0						
		90						

MGF mean grip force, SD standard deviation, SEM standard error of measurement

**Fig. 5** Four representative postures at isometric view. **a** The posture for (0°, 0°, 0°). **b** The posture for (0°, 0°, 90°). **c** The posture for (0°, 70°, 90°). **d** The posture for (90°, 70°, 90°)

both experiments with a sharp decrease. The grip forces for the posture of $(0^\circ, -70^\circ, 0^\circ)$ ‘Major Deflection down’ were slightly bigger than that of the posture of $(0^\circ, 70^\circ, 0^\circ)$ ‘Major Deflection Up’. In other words, the tendencies about five postures were exactly same for the results in this study and actual da Vinci system’s results. From these comparisons, up/down motions of the EndoWrist had a greater effect on grip force than right/left motions.

3.2 Model results and validation

From the Table 1, four randomly chosen measured grip forces were selected to compute the four unknown coefficients shown in Eq. (8) because at least four results of the measured grip force ($F_{M1}, F_{M2}, F_{M3}, F_{M4}$) and four different posture information [$A(\alpha_i, \beta_j, \gamma_k)$] for four different sets of (i, j, k) were required to solve Eq. (8). A set of coefficients: C_0, C_α, C_β , and C_γ was calculated by selecting four results among the 27 results. The remaining 23 grip forces were used to validate the coefficient’s error. This process was repeated with all of the 17,750 sets (${}_{27}C_4 = 17,750$) of coefficients, and the optimal sets for three different EndoWrists with errors are summarized in Table 2. The four different Euler angles for three different EndoWrists shown in Table 2 were used in calculating optimal coefficient among 27 postures in accordance with measured MGF in Table 1. C_0 means that the offset of EndoWrist is oriented by a mechanical characteristic of EndoWrist. Coefficients: C_α, C_β , and C_γ correspond to the roll, pitch, and yaw of the joint characteristics. For the PDF and LND EndoWrist, a set of coefficients with errors of 16.25 and 13.03 % were obtained. Specifically, in the case of PF, the lowest error was calculated as 10.69 %, where the lowest error means that PF EndoWrist is most predictable and less sensitive for the EndoWrist’s posture changes.

4 Discussions

Robotic surgery, an attractive alternative to conventional open and laparoscopic surgery, has been in clinical practice for many years. However, the lack of haptic feedback in current robotic systems was considered to be a limitation that prevented the surgeon from obtaining the sensory information that is desired for enhanced control of the robotic system. Without effective haptic feedback, a surgeon should perform the robotic surgery depending on visual cues and learn by cumulative cases to estimate the force and tension that is placed on tissues and sutures during the surgery. Estimation of the grip forces of the robotic instruments carries clinical significance in this respect.

Mucksavage et al. [12] measured the grip forces of robotic instruments using a 2.2-mm button style compression load cell transducer and a training instrument. These researchers reported that significant differences in the grip force existed between the major deflections compared with the neutral and minor deflections in extended use training instruments. Minor deflections (movements along the distal wrist joint, yawing movements) and the neutral position exhibited a similar grip force, whereas major deflections (movements at the proximal wrist joint, pitching movements) resulted in a significantly lower grip force. It was examined the grip force of the instruments at various angles of EndoWrist’s roll, pitch, and yaw orientations, which are afforded by the seven degrees of freedom. The grip forces were measured for 27 different postures, to predict a quantitative compensation force for the da Vinci end-effector. Table 1 shows that the several grip forces for different postures were different from the overall mean by a minimum of triple the amount. This result was observed when the two postures [14.15 N in $A(90^\circ, 70^\circ, -90^\circ)$ and 4.20 N in $A(-90^\circ, 70^\circ, 90^\circ)$] of the PDF EndoWrist were compared.

Table 2 Optimal coefficient sets of EndoWrists and validation errors

EndoWrist	Angle ($^\circ$)			Coefficients				Error (%)
	Roll (α)	Pitch (β)	Yaw (γ)	C_0	C_1	C_2	C_3	
PF	−90	70	0	15.62	−0.71	−0.65	0.14	10.69
	0	0	−90					
	90	70	−90					
	90	70	90					
PDF	−90	0	0	7.76	1.6	0.42	−0.31	13.03
	−90	70	90					
	90	−70	90					
	90	70	0					
LND	−90	−70	−90	12.23	0.74	−0.54	0.89	16.25
	−90	70	−90					
	−90	70	90					
	90	0	−90					

PF prograsp forceps, PDF PK dissecting forceps, LND large needle driver

This result implies that the additional force, 9.95 N, was required for the posture $A(-90^\circ, 70^\circ, 90^\circ)$, which should be the compensation force for a reliable surgical operation. In Table 1, three EndoWrists' Cronbach's alpha values were greater than, or equal, to the value of 0.99. This meant that the proposed grip force measurement result had an excellent internal consistency [4]. In addition, EIMM was established using the quantitative results. Using EIMM at any posture, a calculation of the compensation force for a reliable surgical operation will be predictable. To evaluate the first-order model proposed in Eq. (7), the errors for the first-order model and the second-order model were computed and compared for the PF EndoWrist, and those were 10.69 and 9.17 %, respectively. Analysis using the high-order term could not reduce the EIMM's prediction error significantly because of the mechanical and nonlinear characteristics of EndoWrist. This observation implies that the first-order model proposed in this study is adequate for the analysis.

Although the proposed optimal coefficient sets did not cover all the ranges of EndoWrist, it could be known which element among the Euler angles created excessive or less force to the EndoWrist. The PF EndoWrist was more affected by the roll and pitch movement of the joint than the yaw. The absolute value of C_α and C_β were greater than C_γ . A surgeon who uses PF EndoWrist should acknowledge that the roll and pitch movement will exceed or loosen the tissue traction. In particular, PDF EndoWrist users should pay attention to the roll movements. The LND EndoWrist was less sensitive to the change in the joint angle compared with the other EndoWrists.

PF EndoWrist exerted a maximum grip force of 20.33 N in $A(0^\circ, 0^\circ, -90^\circ)$, as shown in Table 1. In this posture, approximately 3.50 N (3.65 N and 3.31 N) and 4.50 N (4.07 N and 4.92 N) of the grip force were loosened by changing into a roll movement of 0° to -90° or 0° to 90° and a yaw movement of -90° to 0° or -90° to 90° , respectively. Specifically, almost half of the grip force, 9.00 N (9.28 N and 8.71 N) was lost because of the posture changing the pitch angles 0° to -70° or 0° to 70° . In contrast, 5.50 N (8.10 N and 2.89 N), 4.93 N (9.28 N and 0.57 N), and 2.37 N (2.16 N and 2.58 N) of the excessive grip force were applied to EndoWrist while changing from the posture $A(0^\circ, 70^\circ, -90^\circ)$ to any direction of moving into roll, pitch, and yaw movements. Based on these results, when moving a specific posture to movements of roll, pitch, and yaw, a surgeon should pay special attention to avoid potential damage to tissue. In contrast to the above statement, to avoid a tissue slip incident using EndoWrist, the EndoWrist should be in a reinforced posture, to grab the tissue securely. If the grip forces and the postures were measured and modeled with additional angles based on the EIMM, then the compensation force for any change of angles will be predictable.

Each EndoWrist had a varying set of optimal coefficients and errors for the model because of the tensions on the mechanical strings for gripping motion of EndoWrists were depend on which EndoWrist was used since every EndoWrist's design, mechanism, string interferences, and the EndoWrist's special function, components, and lifespan were subtly different for its own usage. However, because the SDs were significantly small and the values of Cronbach's alpha were estimated as close to the value of 1, grip force results and coefficient using EIMM could be considered to be sufficient to verify that evaluation of the methodology and interpretation of the result were acceptable in this study. To reduce modeling errors, additional combinations of EndoWrist's posture, coupled terms, and lifespan could be considered.

The potential limitations of this study should be addressed as a means for improvement or for mapping out strategies for future study. Knowledge of these differences in the grip force might be unlikely to have any major clinical significance. However, there might be interpersonal variations among learning curves of different surgeons based on their skills and experiences. Understanding the mechanical properties of the robotic system is important to ensure the safe implementation of robotic surgery for less experienced surgeons. The proposed model for EndoWrists had several positive and significant benefits: (1) Surgeon was able to realize the compensation gripping force by EIMM for varying postures (2) if novel TTS using AC servo motor with EIMM were developed, surgeon does not have to consider non-uniform gripping force on laparoscopic robotic surgery because the TTS would calculate the compensation gripping force and compensate the gripping force by exerting torque control (3) continuous calibration using EIMM will resolve the mechanical string's tension issue without any change on EndoWrist's design and mechanism (4) This will greatly increase the safety of the operation procedure.

The developed TTS in this research was different from the da Vinci robot arm's TTS. However, the grip force comparison between the proposed measurement using TTS in this study and actual da Vinci system's results [12] showed an accordant tendency, and the grip forces of three postures $[(0^\circ, 0^\circ, 0^\circ), (0^\circ, 0^\circ, 90^\circ), \text{ and } (0^\circ, 0^\circ, -90^\circ)]$ were also comparable with the actual da Vinci system's results. The amount of values of grip force for the two postures $[(0^\circ, 70^\circ, 0^\circ) \text{ and } (0^\circ, -70^\circ, 0^\circ)]$, which were related to up/down motions, were somewhat different. This was caused by the amount of the differences for deflections between our experiment set-up and the experiment using actual da Vinci system [12]. The amount of deflections about right/left movements of EndoWrist were similar, while it was different for the up/down movements. Although the experimental set-up was unidentical to the real surgical operation, the proposed model and the results from this study are

highly valuable because they provide a grip force analysis and because they predict the grip compensation force without measuring the forces applied to the organs, vessels, or other tissue. The technique also provides the basis for haptic force-feedback modeling and is applicable to other end-effectors, especially scissors, because their shapes and structures are notably similar.

5 Conclusions

The number of surgical operations performed with da Vinci has been rapidly increasing because it has many benefits over the conventional open surgery. However, different grip force for different postures is currently applied, while the surgeon does not recognize the different forces. This issue could lead to a serious accident. In this study, a TTS has been developed to measure the EndoWrist grip forces. It was observed that the measured grip forces for the two different postures differed by 3.37 times (14.15 N vs. 4.20 N). This result means that a compensation force will be required for a safe and reliable operation. To predict the compensation force, a first-order mathematical model of EndoWrist's inner mechanism has been developed, and the model has been validated by comparing the expected grip force from the model with the measured grip force from the da Vinci. This model can be used for EndoWrist grip force analysis and for predicting a compensation model. To apply EIMM to laparoscopic robotic surgery, specific EndoWrist which is used for surgery should be calibrated for those representative several postures before the surgery because changing the mechanical string mechanism and end-effector's design of existing EndoWrist is difficult. With the automatic calibration procedure, the calibration could be done quickly which will lead to the practical use of our methodology.

Acknowledgments This work was partially supported by the Seoul National University Foundation Research Expense (Grant Number: 800-20100525) and a National Research Foundation of Korea (NRF) Grant funded by the Korean Government (Grant Number: 2012-0001638).

References

1. AERA, APA, NCME (1985) Standard for educational and psychological testing. American Psychological Association, Washington
2. Boissy P, Bourbonnais D, Carloti MM, Gravel D, Arsenault BA (1999) Maximal grip force in chronic stroke subjects and

- its relationship to global upper extremity function. *Clin Rehabil* 13:354–362
3. Dobbeltstein JJ, Lee RA, Noorden MV, Dankelman J (2012) Indirect measurement of pinch and pull forces at the shaft of laparoscopic graspers. *Med Biol Eng Comput* 50:215–221
4. George D, Mallery P (2003) SPSS for Windows step by step: a simple guide and reference. Allyn and Bacon, Boston
5. Greenish S, Hayward V, Chial V, Okamura A, Steffen T (2002) Measurement, analysis, and display of haptic signals during surgical cutting. *Presence: Teleoper Virtual Environ* 11:626–651
6. Hashizume M, Konishi K, Tsutsumi N, Yamaguchi S, Shibukuro R (2002) A new era of robotic surgery assisted by a computer-enhanced surgical system. *Surgery* 131:330–333
7. Inc. Intuitive Surgical (2013) The da Vinci surgery experience: over the past decade, more than 1.5 million surgeries have been performed worldwide using the da Vinci Surgical System. Intuitive Surgical. <http://www.davincisurgery.com/assets/docs/da-vinci-surgeryfact-sheet-en-1005195.pdf?location=1&version=b>. Accessed 19 Sept 2014
8. Inc. maxon motor. Maxon DC motor: Maxon motor Inc. http://www.engr.ucsb.edu/~mdnip/me170c/datasheets/25mm_Motors.pdf. Accessed 19 Sept 2014
9. Johnson PJ, Schmidt DE, Duvvuri U (2014) Output control of da Vinci surgical system's surgical graspers. *J Surg Res* 186(186):56–62
10. King CH, Culjat MO, Franco ML, Lewis CE, Dutson EP, Grundfest WS, Bisley JW (2009) Tactile feedback induces reduced grasping force in robot-assisted surgery. *IEEE T Haptics* 2:103–110
11. Mosse CA, Mills TN, Bell GD, Swain CP (1998) Device for measuring the forces exerted on the shaft of an endoscope during colonoscopy. *Med Biol Eng Comput* 36:186–190
12. Mucksavage P, Kerbl DC, Pick DL, Lee JY, McDougall EM, Louie MK (2011) Differences in grip forces among various robotic instruments and da Vinci surgical platforms. *J Endourol* Mar 25:523–528
13. Ortmairer T, Hirzinger G (2000) Cartesian control issues for minimally invasive robot surgery. *Intell Robots Syst (IROS 2000)*. Proceedings 2000 IEEE/RSJ international conference on; 2000:565–572
14. Park SY, Cho KS, Lee SW, Soh BH, Rha KH (2008) Intraoperative breakage of needle driver jaw during robotic-assisted laparoscopic radical prostatectomy. *Urology* 71:168-e5–168-e6
15. Ruegg M (2010) Application note medical technology: surgical robots for minimally invasive procedures. Maxon motor ag. http://www.maxonmotor.com.au/downloads/Servo_motor_and_gearhead_in_Surgical_Robotics.pdf. Accessed 19 Sept 2014
16. Seibold U, Kubler B, Hirzinger G (2005) Prototype of instrument for minimally invasive surgery with 6-axis force sensing capability. *Robotics and automation, 2005 ICRA 2005 proceedings of the 2005 IEEE international conference on* 2005:18–22
17. Sung GT, Gill IS (2001) Robotic laparoscopic surgery: a comparison of the da Vinci and Zeus systems. *Urology* 58:893–898
18. Tavakoli M, Patel RV, Moallem M (2005) Haptic interaction in robot-assisted endoscopic surgery: a sensorized end-effector. *Int J Med Robot Comput Assist Surg* 1:53–63